O'Brien, M. P., and R. G. Folsom, "The Transportation of Sand in Pipe Lines," *Univ. Calif. Pub. Eng.*, 3, No. 7, 343-384 (1937).
Rother, E. G., "Hydraulic Transportation of Solids in Horizontal Pipelines," M.S. thesis, Col. School of Mines (May, 1959).
Schriek, W., L. G. Smith, D. B. Haas, and W. H. W. Husband, "The Potential of Helically Ribbed Pipes for Solids Transport," *Can. Min. Met. Bull.*, 1-8 (Oct., 1974).
Shih, C. C. S., "Hydraulic Transport of Solids in a Sloped Pipe," *J. Pipeline Div. ASCE*, 90, No. PL2, P. Paper 4125, 1-14 (1964).
Smith, L. G., W. Schriek, W. H. W. Husband, and C. A. Shook, "Pilot-Plant Facilities for Hydraulic Transport of Solids," *Can. Min. Met. Bull.*, 1-3 (June, 1973).
Smith, R. A., "Experiments on the Flow of Sand-Water Slurries in Horizontal Pipes," *Trans. Inst. Chem. Engrs.*, 33, 85-92 (1955).
Soleil and Ballade, "Hydraulic Transport of Solids in Public Works," *2e Journees d'Hydraulique Societe Hydrotechnique de France*, Grenoble (June, 1952).
Spells, K. E., "Correlations for Use in Transport of Aqueous Suspensions on Fine Solids through Pipes," *Trans. Inst. Chem. Engrs.*, 33, 79-84 (1955).
Thomas, D. G., "Transport Characteristics of Suspensions:VI, Minimum Transport Velocity for Large Particle Size Suspensions in Round Horizontal Pipes," *AIChE J.*, 8, 373-378 (1962).
Turian, R. M., T. F. Yuan, and G. Mauri, "Pressure Drop Correlation for Pipeline Flow of Solid-Liquid Suspensions," *ibid.*, 17, 809-817 (1971).
Vocadlo, J. J., and M. S. Sagoo, "Slurry Flow in Pipes and Pumps," *J. Eng. Ind.*, 95, 65-71 (Feb., 1973).
Wasp, E. J., T. C. Aude, J. P. Kenny, R. H. Seiter, P. B. Williams, and R. B. Jacques, "Deposition Velocities and Spatial Distribution of Solids in Slurry Pipelines." presented at the 1st International Conference on the Hydraulic Transport of Solids in Pipes, Coventry, England (Sept., 1970).
Wilson, W. E., "Mechanics of Flow, with Noncolloidal, Inert Solids," *Trans. ASCE*, 107, 1576-1594 (1942).
Worster, R. C., and D. F. Denny, "Hydraulic Transport of Solid Material in Pipes," *Proc. Inst. Mech. Engrs.*, 169, 563-586 (1955).
Yuan, T. F., "Liquid-Solid Suspension Flow in Horizontal Pipes," Ph.D. dissertation, Syracuse Univ., New York (1971); *Dissert. Abstr. Intern.*, 33, 181 B (1972).
Zandi, I., ed., *Advances in Solid-Liquid Flow in Pipes and Its Application*, Pergamon Press, N.Y. (1971).
———, and G. Govatos, "Heterogeneous Flow of Solids in Pipelines," *J. Hydr. Div., ASCE*, 93, H'Y 3, 145-159 (1967).

Manuscript received September 22, 1976; revision received January 12, and accepted January 13, 1977.

Use of Trajectory Analysis to Study Stability of Colloidal Dispersions in Flow Fields

G. R. ZEICHNER
and
W. R. SCHOWALTER
Department of Chemical Engineering
Princeton University
Princeton, New Jersey 08540

Trajectories have been computed for two equal sized spherical particles in simple laminar shearing and in uniaxial extensional flows. Effects of interparticle attraction, electrostatic repulsion, and hydrodynamics were included.

The results are pertinent to questions of colloidal stability under various conditions of flow. Particulate dispersions can react in several different ways as the intensity of shearing is increased from zero: the dispersion can remain stable; it can be redispersed, if it had been initially flocculated into a weak secondary minimum in the interparticle potential curve; it can be flocculated into a strong primary minimum in the potential curve; or, in extreme cases, it can be redispersed from the primary minimum. Results are presented which illustrate criteria for flocculation or stability to both laminar shearing and extensional flow. It is shown that hydrodynamic effects can significantly alter the criteria developed for stability of dispersions to Brownian coagulation.

SCOPE

Colloidal stability, by which one means the tendency of a suspension to remain dispersed and to resist flocculation, is dependent on many factors. These include the actions of Brownian motion, London attractive forces, electrostatic repulsive forces, and hydrodynamic forces, the latter being generated by bulk motion of the suspension. It is desirable to know how these various forces combine to promote stable or unstable dispersions. The factors which affect colloidal stability are important to those, such as manufacturers of polymer latices, who wish to insure stability, and also to those who wish to flocculate particulate suspensions, thereby separating finely divided solids from a liquid.

In the present study, the trajectories of two equal sized spherical particles in simple laminar shearing and in a uniaxial extensional flow were analyzed. In addition to the action of hydrodynamic forces, the effects of London attraction and electrostatic repulsion were calculated. Brownian motion was excluded from the trajectory analysis, but its effects were considered separately,

as in the previous work of Swift and Friedlander (1964). From the results one can calculate the probability that two spheres, initially independent of each other, will form a dynamic system in which the spheres remain in close proximity and, hence, are captured. One can ascertain both the kinetics and the ultimate degree of stability of a colloidal dispersion, given appropriate initial conditions.

Prior work on stability has either been concerned only with Brownian motion or has included flow only in a restricted context (Utracki, 1973).* This is because it is only recently that a general trajectory analysis has been developed for two spheres in creeping flow (Batchelor and Green, 1972).

CONCLUSIONS AND SIGNIFICANCE

Correction of Smoluchowski's theory of coagulation rates to include the effect of hydrodynamic forces reduces, somewhat, the dependence of particle collision rate on the flow strength. In laminar shearing, for example, the collision rate dependence on shear rate changes from a direct proportion to a 0.77 power dependence. The collision rate is dependent on the type of fluid motion to which a suspension is subjected. In the high flow strength limit, extensional flow is more efficient for the purposes of flocculation.

Shearing forces can act either to flocculate or to disperse a suspension of particles, and flocculation can occur in either a primary or secondary minimum of a curve representing interparticle potential. Stability criteria for both shearing and extensional flow were determined. The results for these two flows are superposable by a suitable transformation of the flow strength axis.

When the criteria for stability to only shearing forces are compared with the criteria for stability to only Brownian forces, it is shown that, for cases of interest, shearing forces can have a substantial effect on the overall stability of a suspension. This prediction is consistent with experiments.

The interplay between colloidal and hydrodynamic effects in a flowing suspension has been demonstrated. The results illustrate how shearing can, under some conditions, induce flocculation and under others promote dispersion. The fact that vorticity and deformation rate separately affect flocculation is an important consideration for design of flow systems which enhance or inhibit flocculation.

The results have significance beyond the usual questions of colloid stability. The rheology of suspensions depends, of course, on the distribution of particulate matter throughout the continuous phase. Colloidal and shearing forces can alter that distribution and, hence, can affect the rheology of the suspension.

Encounters between particles in a colloidal suspension occur because of random Brownian motion, even though the suspension as a whole is at rest. If electrostatic or steric barriers exist that are sufficiently larger than the average thermal energy of a Brownian particle, the suspension can remain stable for a period of years. A theory that describes the interplay between these forces is known as the DLVO theory because of its development, independently, by Derjaguin and Landau (1941) and Verwey and Overbeek (1948). The DLVO theory is used in the present work to describe nonhydrodynamic forces.

The first analysis of kinetics of Brownian coagulation was that of von Smoluchowski (1917), who assumed that repulsive forces were negligible. This condition is often referred to as rapid flocculation in the literature. He used a simple diffusion model to calculate the rate of collisions. Hydrodynamic interactions were neglected, and particle-particle influence was modeled by a sticking force for particles in contact. Improvements to von Smoluchowski's theory, through the inclusion of an arbitrary interparticle force and hydrodynamic interactions, only affect the collision rate by a multiplication factor $1/W$, first introduced by Fuchs (1934). The factor W has acquired the name stability ratio because it allows one to be quantitatively specific about the meaning of stability. From von Smoluchowski's kinetic analysis, the time required for the total number of particles to be halved is

$$t = \frac{3\mu}{4kTN_o} W \qquad (1)$$

Given a repulsive force for which $W = O(10^5)$, a dilute suspension in water would be expected to be stable for weeks. Verwey and Overbeek (1948) recognized the importance of W and, using DLVO theory, reported extensive calculations of the stability ratio.

The descriptions cited above are for systems in which there is no bulk motion. In the presence of flow, particle-particle encounters are also caused by hydrodynamic forces. These flow induced encounters, which can significantly enhance the coagulation rate, are potentially useful in water pollution control and in recovery processes where the removal of particulates is desirable. Suspensions that resist flow induced coagulation are said to be mechanically stable. Although flow induced coagulation has been experimentally verified and studied (Stamberger, 1962; Swift and Friedlander, 1964; Utracki, 1973; Green and Sheetz, 1970; Roe and Brass, 1955), it has not received as much theoretical attention as has Brownian coagulation.

Neglecting Brownian motion and hydrodynamic complexities, von Smoluchowski (1917) calculated the rate of collisions in a shear field for particles with only a sticking force on contact. In analogy to Brownian coagulation, described by Equation (1), von Smoluchowski's result can be extended by inclusion of hydrodynamics and an arbitrary potential. The collision rate is altered by a factor $1/W$, where W is interpreted here as a stability ratio for flow induced coagulation. Using von Smoluchowski's kinetics for a shear flow, the total number of particles is halved in the time

$$t = \frac{0.173\pi}{\dot{\gamma}\,\phi_p} W \qquad (2)$$

where $\dot{\gamma}$ is the shear rate and ϕ the volume fraction.

* In a paper which appeared after the present work was submitted, Van de Ven and Mason (1976) have calculated particle trajectories by a technique similar to ours. However, they are concerned solely with particle trajectories in laminar shearing and do not consider elongational flow.

Curtis and Hocking (1970) were the first to include hydrodynamic interactions in the calculation of shear induced coagulation. They were interested in determining the Hamaker constant from a rapid flocculation experiment, and, consequently, they only considered London attractive forces.

In the work reported here, a rather general treatment (Batchelor and Green, 1972) has been employed to describe hydrodynamic effects. Both repulsive and attractive interparticle forces have been incorporated into the calculations. Specific stability criteria are presented and compared for laminar shear flow and for uniaxial extensional flow. As in previous studies, the analysis is restricted to sufficiently dilute systems so that only two-body interactions are important.

INTERPARTICLE FORCES

Dispersions of small particles exhibit a wide variety of behavior attributable to short-range interparticle forces. Flocculation and the formation of strongly bound aggregates are the most obvious manifestations of these forces. However, they are also responsible for such non-Newtonian behavior as shear thinning, yield stresses, dilatancy, rheopexy, and thixotropy.

The interparticle force is the sum of an attractive, London force and a repulsive electrical double-layer force. The total potential energy of interaction V_T is a function of the interparticle separation and, when the repulsive force is significant, has the general shape shown in Figure 1. Given appropriate magnitudes of the repulsive barrier V_{max} and the depth of the secondary minimum well V_{sec}, three stability regimes can be identified. One regime corresponds to an interaction energy dominated by attraction so that particles rapidly flocculate to form large, strong aggregates. Because of the deep minimum in the interaction potential at small separations, particles flocculated into this primary minimum are difficult, if not impossible, to redisperse. In another regime the electrical repulsive barrier V_{max} prohibits primary minimum flocculation; however, the longer-range attractive force causes flocculation into a weak secondary minimum, V_{sec}. Both Schenkel and Kitchener (1960) and Kotera, Furusawa, and Kudō (1970) have experimentally verified the existence of secondary minimum flocculation in latex suspensions. Lastly, particles can remain well dispersed when repulsive forces are large enough to reduce the secondary minimum significantly.

The London force between particles was first calculated by Hamaker (1937), who assumed pairwise additivity of the intermolecular interactions. For equal sized spheres, he found

$$V_A = -\frac{A}{6}\left[\frac{2}{R^2-4}+\frac{2}{R^2}+\ln\left(\frac{R^2-4}{R^2}\right)\right] \tag{3}$$

where $R = r/a$ is the dimensionless separation between sphere centers. The effect of the dispersing medium is included in the value of the Hamaker constant A. Because electromagnetic retardation was neglected, Hamaker's expression is only valid for separations less than the London wavelength λ_L (typically, 0.1 μm). Schenkel and Kitchener (1960) included retardation and reported the following best-fit approximations to their numerical integrations for $R - 2 << 1$:

$$V_A \cong \frac{A}{R-2}\left[\frac{-2.45}{60p_o}+\frac{2.17}{180p_o^2}-\frac{0.59}{420p_o^3}\right]$$

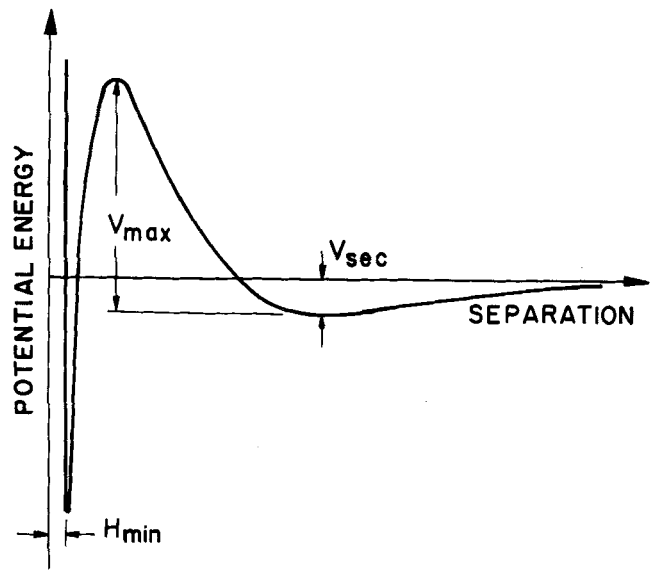

Fig. 1. Schematic drawing of interparticle potential energy.

for $p_o > 0.57$ (4a)

$$V_A \cong \frac{-A}{12(R-2)}\left[\frac{1}{1+1.77p_o}\right] \quad \text{for } p_o \leq 0.57 \tag{4b}$$

where $p_o = 2\pi(R-2)/\alpha$, and $\alpha = \lambda_L/a$. The dimensionless parameter α determines the degrees of retardation, the limit $\alpha \to \infty$ corresponding to the unretarded case. For all of the calculations reported here, Equations (3) and (4) have been used, respectively, for unretarded and retarded attractive forces.

Several of the assumptions inherent in Hamaker's theory are open to question, the most notable being pairwise additivity of intermolecular potentials. Although this assumption can be avoided in the more rigorous continuum theory of Lifshitz (1955), the recent calculations of Evans and Napper (1973) and Smith, Mitchell, and Ninham (1973) suggest that the potential functions of Schenkel and Kitchener are adequate, provided that the Hamaker constant is either calculated from the Lifshitz theory or measured experimentally.

Electrical double-layer interactions can conceivably occur such that either the surface potential ψ_o or the surface charge density σ_o remains constant. If particle-particle encounters are sufficiently slow, redistribution of the surface charge will maintain an electrostatic equilibrium, and the surface potential will be constant. Frens and Overbeek (1972), however, argue that during the time scale of a Brownian encounter, the diffusion of ions necessary to maintain electrostatic equilibrium will be sufficiently slow so that encounters will occur at constant surface charge rather than constant surface potential.

If we accept the Gouy-Chapman description of the electrical double layer (Verwey and Overbeek, 1948), several approximations are needed to obtain an analytical solution for the double-laver interactions of two spherical particles. The following interaction potentials were derived for thin double lavers ($\tau = a\kappa > 10$), low surface potentials ($ez_i\psi_o/kT < 2$), and symmetrical electrolytes:

$$V_R = \frac{\epsilon\psi_o^2 a}{2}\ln\{1 \pm \exp[-\tau(R-2)]\} \tag{5}$$

The + and − correspond, respectively, to the constant surface potential solution of Derjaguin and Landau (1941) and the constant surface charge solution of Frens and

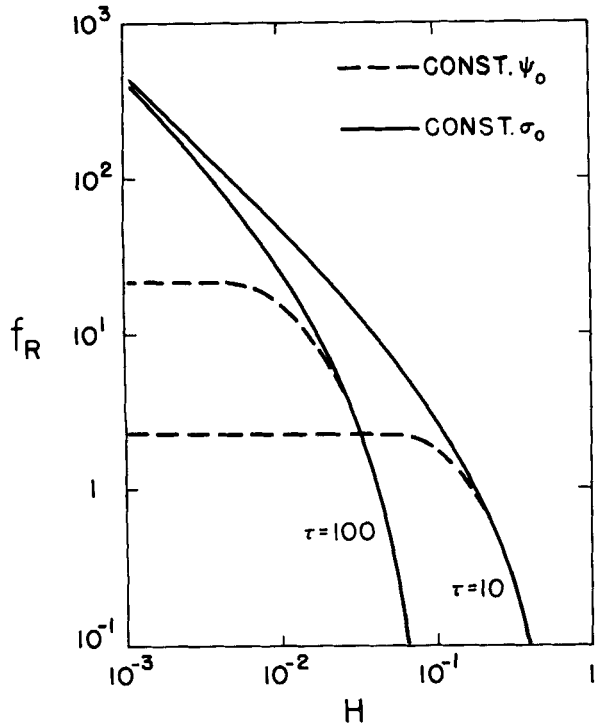

Fig. 2. Comparison of the repulsive forces obtained for the boundary conditions: constant ψ_o and constant σ_o.

Overbeek (1972). For the constant surface charge solution, the surface potential ψ_o is interpreted as the surface potential of a single particle alone in the fluid and is related to the surface charge density by

$$\psi_o = \frac{4\pi a \sigma_o}{\epsilon(1+\tau)} \tag{6}$$

The zeta potential obtained from electrophoretic mobility of a particle is commonly used as an approximation of the surface potential ψ_o. The two force expressions obtained from Equations (5) are shown in Figure 2, where the dimensionless force

$$f_R = -\frac{1}{\epsilon\psi_o^2}\frac{dV_R}{dr} \tag{7}$$

is plotted as a function of the dimensionless minimum distance between particle surfaces, $H = (R - 2)$.

Bell and Peterson (1972) have compared Equation (5) to more exact numerical solutions. For $ez_i\psi_o/kT \leq 2.0$, errors of less than 10% were found for the constant ψ_o case, whereas errors of 500% were found for the constant σ_o case. The larger error for the constant σ_o solution occurs because the surface potential increases without bounds as the separation decreases, thus invalidating the restriction to low surface potentials. In using the potential based on constant surface charge, an overestimate of the stability of the suspension is, therefore, expected.

An additional repulsive force is present at separations for which electron clouds begin to overlap. These forces are approximated by $V \to \infty$, and they limit the separation between particle surfaces to some minimum value. For smooth particles with clean surfaces, the minimum separation distance is typically 4Å. Adsorbed surfactants or marcromolecules can, however, increase the minimum separation to as much as 100Å.

The total force acting on the particles is obtained by summing the attractive and repulsive contributions:

$$F_c = -\frac{d}{dr}(V_A + V_R) \tag{8}$$

Introducing the dimensionless functions $f_R(R, \tau)$, defined in Equation (7), and

$$f_A(R, \alpha) = -\frac{a}{A}\frac{dV_A}{dr} \tag{9}$$

we can express the total force as

$$F_c = \infty \quad \text{for} \quad R = (2 + H_{\min}) \tag{10a}$$

$$F_c = \frac{A}{a}[f_A(R, \alpha) + N_R f_R(R, \tau)] \quad \text{for} \quad R > (2 + H_{\min}) \tag{10b}$$

where $N_R = \epsilon\psi_o^2\, a/A$. The value of N_R indicates the importance of the repulsive force relative to the attractive force.

TWO-SPHERE HYDRODYNAMICS

In this section, the relative motion of two Brownian particles acted upon by interparticle forces is described. The pair is assumed to be alone in a fluid of infinite extent. The fluid may undergo a bulk motion $\mathbf{u}_o$ that varies linearly in space. This flow is described by a constant deformation rate tensor

$$\mathbf{E} = \frac{1}{2}[\nabla \mathbf{u}_o + (\nabla \mathbf{u}_o)^T] \tag{11}$$

and a constant angular velocity

$$\boldsymbol{\omega} = \frac{1}{2}(\nabla \times \mathbf{u}_o) \tag{12}$$

For low Reynolds number flows, typical of colloidal suspensions, the flow field $\mathbf{u}$ in the presence of the particles is adequately described by the creeping motion equations:

$$\nabla \cdot \mathbf{u} = 0 \tag{13a}$$

$$\mu\nabla^2\mathbf{u} = \nabla p \tag{13b}$$

The no-slip condition requires that

$$\mathbf{u} = \mathbf{U}^I + \boldsymbol{\Omega}^I \times \mathbf{R}^I \quad \text{on the surface of sphere } I$$

$$\mathbf{u} = \mathbf{U}^{II} + \boldsymbol{\Omega}^{II} \times \mathbf{R}^{II} \quad \text{on the surface of sphere } II$$

where $\mathbf{U}^I$ and $\mathbf{U}^{II}$ denote the translational velocities of the spheres, $\boldsymbol{\Omega}^I$ and $\boldsymbol{\Omega}^{II}$ denote the angular velocities of the spheres about their centers, and $\mathbf{R}^I$ and $\mathbf{R}^{II}$ are position vectors of the sphere surfaces relative to their respective centers. Far from the particles any hydrodynamic disturbances die out, and $\mathbf{u} \to \mathbf{u}_o$.

The unknown translational and angular velocities of the spheres are determined by a force and torque balance on each particle. In the absence of gravitational effects and external fields, colloidal particles experience three forces: a hydrodynamic force

$$\mathbf{F}_{\text{hyd}} = \int_{A_p} \boldsymbol{\sigma} \cdot \mathbf{n} dS \tag{14}$$

where $\boldsymbol{\sigma} = -p\mathbf{I} + \mu[\nabla\mathbf{u} + (\nabla\mathbf{u})^T]$, an interparticle force $\mathbf{F}_c$, and a thermodynamic force due to the Brownian process. This latter force is a statistical one for which it is necessary to introduce the pair probability function for the separation between two particles $P(\mathbf{r}, a/b)$. Provided that the statistical properties of the suspension are homogeneous throughout space, the pair probability function is independent of position. The probability that the center of a particle with radius b will be in some element of volume $d\mathbf{r}$ centered at distance $\mathbf{r}$ from the center of a particle with

radius a is

$$P(\mathbf{r}, a/b)dr$$

When integrated over all space

$$n_b \int P(\mathbf{r}, a/b)dr = N_b \tag{15}$$

where N_b refers to the total number of particles with radius b and n_b to the corresponding number density. The Brownian force exerted on the pair is (Batchelor, 1976)

$$\mathbf{F}_{Br} = -kT\nabla \ln P(\mathbf{r}, a/b) \tag{16}$$

Neglecting inertia, one can write $\mathbf{F}_{hyd} + \mathbf{F}_c + \mathbf{F}_{Br} = 0$. The particles are assumed torque free, so that

$$\mathbf{T}_{\text{hyd}} = \int_{A_p} \mathbf{r} \times (\boldsymbol{\sigma} \cdot \mathbf{n})dS = 0 \tag{17}$$

where the integration is over the surface of any particle. From the solution to the above system of equations, the relative velocity of the pair $\mathbf{v} = \mathbf{U}^{II} - \mathbf{U}^{I}$ is obtained.

Linearity of the creeping motion equations permits decomposition of the velocity field into three independent and superposable motions:

$$\mathbf{u} = \mathbf{u}_{\text{flow}} + \mathbf{u}_{F_c} + \mathbf{u}_{Br} \tag{18}$$

The velocity field $\mathbf{u}_{\text{flow}}$ is chosen to be that caused by the motion of two force free spheres in the undisturbed linear flow field $\mathbf{u}_o$. Then, from a solution of the creeping motion equations for $\mathbf{F}_{\text{hyd}} = \mathbf{T}_{\text{hyd}} = 0$, one can obtain an expression for the velocity of one particle relative to the other in the form given by Batchelor and Green (1972):

$$\mathbf{v}_{\text{flow}} = \boldsymbol{\omega} \times \mathbf{r} + \mathbf{E} \cdot \mathbf{r} - \left\{ \mathcal{A}(R)\frac{\mathbf{rr}}{r^2} + \mathcal{B}(R)\left(\mathbf{I} - \frac{\mathbf{rr}}{r^2}\right)\right\} \cdot \mathbf{E} \cdot \mathbf{r} \tag{19}$$

where the parameters $\mathcal{A}$ and $\mathcal{B}$ are independent of the nature of the linear flow field and are functions only of the nondimensional separation and the ratio of the particle sizes. Unfortunately, numerical values of $\mathcal{A}$ and $\mathcal{B}$ are only known from the bispherical coordinate solution of Lin et al. (1970) for equal sized spheres. Because of the singularity in the bispherical coordinate system for nearly touching spheres, Lin's solution must be augmented by the lubrication approximation of Batchelor and Green (1972). Curtis and Hocking (1970) used a bispherical coordinate solution similar to Lin's but evidently did not apply the lubrication approximation at small separations.

The second velocity field $\mathbf{u}_{F_c}$ is selected to be that due to the motion along the line of centers of two particles in a quiescent fluid acted upon by the force $\mathbf{F}_c$. The solution to this problem was obtained by Maude (1961) and can be expressed as

$$\mathbf{v}_{F_c} = \frac{\mathcal{G}(R)F_c\mathbf{e}_r}{6\pi\mu a} \tag{20}$$

The correct series solution for $\mathcal{G}(R)$ is contained in Spielman (1970) and is related to his quantity $f(r)$ by $\mathcal{G}(R) = 6\pi\mu a f(r)$.

The values of $\mathcal{A}(R)$, $\mathcal{B}(R)$, and $\mathcal{G}(R)$ are contained in Table 1 for equal sized spheres. To interpolate between these values, the data in Table 1 were fitted with cubic splines. However, for $R < 2.0001$, B was evaluated using the asymptotic expression of Batchelor and Green (1972): $B = 0.4060 + 0.78/\ln H$. The function $\mathcal{G}/(1 - \mathcal{A})$, which will be of use later, is also presented in Table 1 for several values of R. This quantity should decrease monotonically to a value of unity. Because the function $\mathcal{G}$ was found,

Table 1. Functions for Equations (19) and (20)

R	$\mathcal{A}$	$\mathcal{B}$	$\mathcal{G}$	$\mathcal{G}/(1-\mathcal{A})$
2.0000	1.0000	0.4060	0	1.000
2.0001	0.9996	0.3213	0.0004	1.000
2.0025	0.9900	0.2762	0.0098	0.980
2.0100	0.9619	0.2461	0.0374	0.980
2.0401	0.8679	0.1996	0.1310	0.990
2.0907	0.7505	0.1608	0.2510	1.006
2.1621	0.6313	0.1275	0.3777	1.024
2.2553	0.5214	0.0988	0.5017	
2.3709	0.4248	0.0748	0.6190	
2.5103	0.3424	0.0553	0.7287	
2.6749	0.2735	0.0399	0.8306	
2.8662	0.2167	0.0281	0.9254	
3.0862	0.1704	0.0193	1.0133	
3.3370	0.1331	0.0130	1.0950	
3.6213	0.1033	0.00856	1.1709	
4.7048	0.0468	0.0023	1.3666	
6.2149	0.0204	0.0006	1.5207	
11.1139	0.0036	0.0000	1.7310	
20.1353	0.0006	0.0000	1.8512	

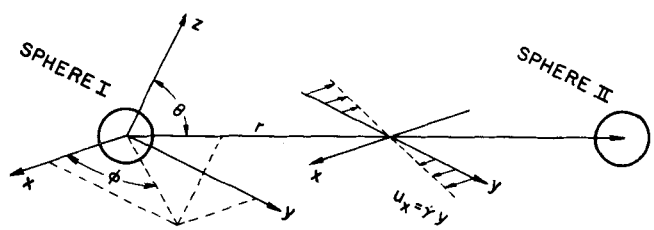

Fig. 3. Coordinates for trajectory equations.

with negligible truncation error, from a series solution, the discrepancy of the several values less than unity is probably a measure of the truncation error involved in Lin's numerical calculations.

The third flow $\mathbf{u}_{Br}$ engendered by two Brownian particles in a quiescent fluid contributes a relative velocity (Batchelor, 1976) of the form

$$\mathbf{v}_{Br} = -\mathbf{D}(r) \cdot \nabla \ln P(\mathbf{r}, a/b) \tag{21}$$

where the relative diffusion tensor $\mathbf{D}(r)$ is a function of separation and particle size ratio. The relationship between $\mathbf{D}(r)$ and the relevant hydrodynamic mobilities of a pair of particles is available from Batchelor (1976). The total relative velocity of the pair is the sum of the contributions made by each of these flow fields:

$$\mathbf{v} = \mathbf{v}_{\text{flow}} + \mathbf{v}_{F_c} + \mathbf{v}_{Br} \tag{22}$$

The relative trajectory of a pair of colliding particles will be needed for determination of the flow induced coagulation rate. Brownian motion will be neglected for the moment $\mathbf{v}_{Br} = 0$, so the trajectory of a pair is uniquely determined from an initial configuration. The trajectories are described in a moving coordinate system (x, y, z) with fixed orientation in space and an origin embedded in the center of sphere I. The center of sphere II is located relative to this coordinate system by the spherical coordinates (r, θ, ϕ), where $\theta = 0$ corresponds to the positive z axis, as shown in Figure 3.

The trajectory equations which describe the relative rate of change of the position of sphere II are given by the spherical components of the relative velocity $\mathbf{v} = \mathbf{v}_{\text{flow}} + \mathbf{v}_{F_c}$. For plane Couette flow with the orientation shown in Figure 3

$$[\mathbf{E}] = \begin{bmatrix} 0 & \dot{\gamma}/2 & 0 \\ \dot{\gamma}/2 & 0 & 0 \\ 0 & 0 & 0 \end{bmatrix} \; ; \quad \boldsymbol{\omega} = (0, 0, -\dot{\gamma}/2)$$

and the dimensionless trajectory equations are

$$\frac{dR}{dt^0} = (1 - \mathcal{A})R\sin^2\theta\sin\phi\cos\phi + \frac{\mathcal{G}}{N_F}(f_A + N_R f_R) \tag{23a}$$

$$\frac{d\phi}{dt^0} = \sin^2\phi + \frac{1}{2}\mathcal{B}(\cos^2\phi - \sin^2\phi) \tag{23b}$$

$$\frac{d\theta}{dt^0} = (1 - \mathcal{B})\sin\theta\cos\theta\sin\phi\cos\phi \tag{23c}$$

where $t^0 = \dot{\gamma}\, t$ and $N_F = 6\pi\mu a^3\dot{\gamma}/A$. For both a uniaxial extensional flow with the principal elongation along the z axis and

$$[\mathbf{E}] = \begin{bmatrix} -\dot{\gamma} & 0 & 0 \\ 0 & -\dot{\gamma} & 0 \\ 0 & 0 & 2\dot{\gamma} \end{bmatrix} \; ; \quad \boldsymbol{\omega} = (0, 0, 0)$$

and the reverse flow, a uniaxial compression, with

$$[\mathbf{E}] = \begin{bmatrix} \dot{\gamma} & 0 & 0 \\ 0 & \dot{\gamma} & 0 \\ 0 & 0 & -2\dot{\gamma} \end{bmatrix} \; ; \quad \boldsymbol{\omega} = (0, 0, 0)$$

the dimensionless trajectory equations are of the form

$$\frac{dR}{dt^0} = \pm(1 - \mathcal{A})R\,(3\cos^2\theta - 1) + \frac{\mathcal{G}}{N_F}(f_A + N_R f_R) \tag{24a}$$

$$\frac{d\theta}{dt^0} = \pm 3(1 - \mathcal{B})\sin\theta\cos\theta \tag{24b}$$

$$\frac{d\phi}{dt^0} = 0 \tag{24c}$$

The + and − correspond, respectively, to extensional and compressional flow.

The trajectory equations were integrated numerically using an algorithm of Merson (Christiansen, 1970). In the absence of interparticle colloidal forces where $N_F = \infty$, the numerical results for shear flow can be compared with the analytical solution of Lin et al. (1970). For a given trajectory, the error in the numerical solution for the separation $H = (R - 2)$ as a function of θ was at most 2%.

COAGULATION RATES AND THE STABILITY RATIO

The coagulation process, as conceived by von Smoluchowski, is modeled by two-body collisions that cause the destruction of the colliding pair and the creation of a new particle with mass equivalent to that of the pair. The disappearance of two particles with radii a and b will occur at the collision surface $r = a + b$, and, therefore

$$P(\mathbf{r}, a/b) = 0 \quad \text{for} \quad r = a + b \tag{25}$$

At large separations, hydrodynamic and interparticle forces vanish, so no long-range order is expected and any configuration of the pair is equally likely. Provided that all particle-particle encounters originate at infinite separation such that there are no regions of closed trajectories

$$P(\mathbf{r}, a/b) \to 1 \quad \text{as} \quad r \to \infty \tag{26}$$

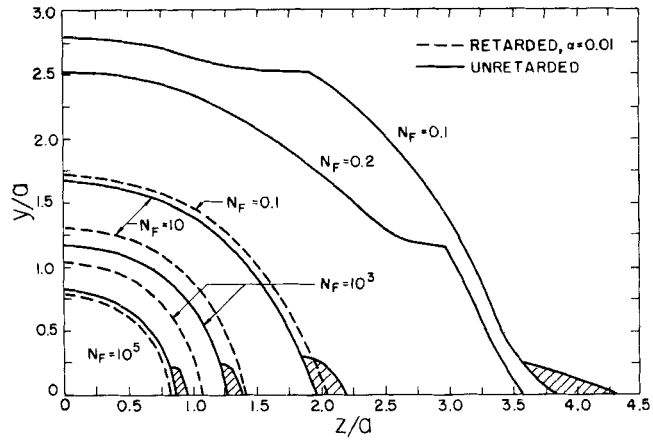

Fig. 4. Upstream interception areas for shear flow determined for both an unretarded attractive force, Equation (3), and a retarded force, Equation (4). The shaded region corresponds to collisions for the unretarded case which occur in more than one-half rotation, $\phi > 180$ deg, but not more than one complete rotation, $\phi \leq 360$ deg.

In the absence of interparticle forces, a region of closed trajectories exists for shear flow in which particles orbit one another as a permanent doublet. For the limiting open trajectory in the plane $\theta = 90$ deg that separates the region of open trajectories from the region of closed trajectories, the minimum separation between identical particles is $H = 4.5 \times 10^{-5}$ at $\phi = 90$ deg. The interparticle force $\mathbf{F}_c$, discussed earlier, is significant at separations much greater than this and must be considered. For forces typical of colloidal systems, trajectory calculations indicate that particles in the region of what would be closed trajectories in the absence of interparticle forces are either coagulated or repulsed into an open trajectory after initiation of flow. Therefore, encounters can be taken to originate at infinite separation.

For the dilute suspension being considered here, the pair probability function is taken to be independent of the coagulation process. In the region defined by $(a + b) < r < \infty$, the probability that a given pair will have a configuration in the range between $\mathbf{r}$ and $\mathbf{r} + d\mathbf{r}$ is a conserved quantity, and application of the Reynolds transport theorem provides the governing equation for the pair probability function in this region:

$$\frac{\partial P}{\partial t} + \nabla \cdot (\mathbf{v}P) = 0 \quad \text{for} \quad (a + b) < r < \infty \tag{27}$$

The velocity $\mathbf{v}$ is simply the relative velocity of the sphere centers, given by Equation (22). The familiar diffusion equation is obtained by substituting the solution obtained for the relative velocity into Equation (27) and writing the equation in dimensionless form:

$$\frac{\partial P}{\partial t^0} + \nabla \cdot \left\{ \left[\mathbf{v}'_{\text{flow}} + \frac{\mathcal{G}}{N_F}\left[f_A(R, \alpha) + N_R f_R(R, \tau) \right] \mathbf{e}_r \right] P \right\} = \frac{1}{N_{Pe}} \nabla \cdot [\mathbf{D}' \cdot \nabla P] \tag{28}$$

where

$$\mathbf{D}'(R) = \frac{6\pi\mu a}{kT}\mathbf{D}(r)$$

and

$$N_{Pe} = \frac{6\pi\mu a^3\dot{\gamma}}{kT}$$

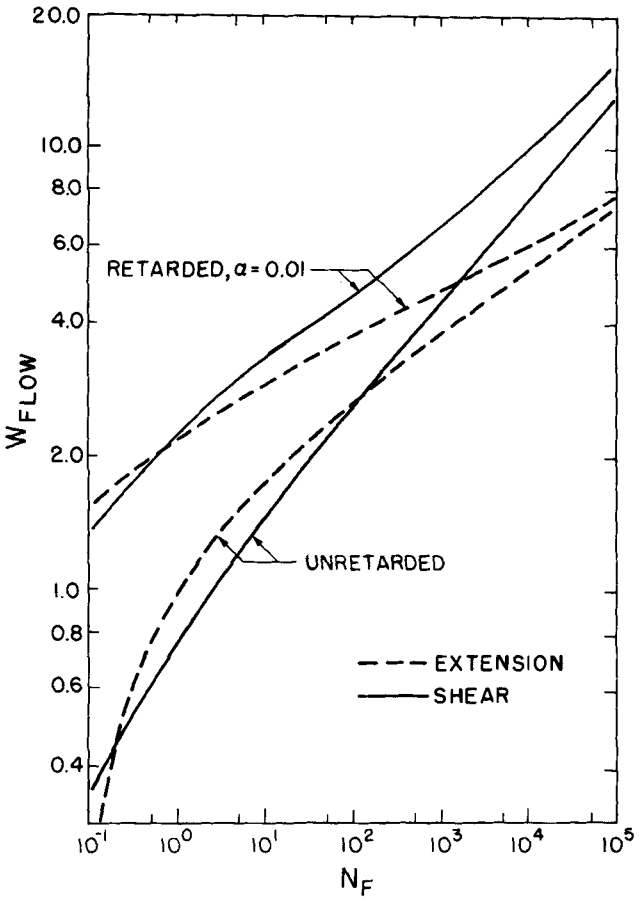

Fig. 5. The stability ratio for both shear and extensional flow in the absence of repulsive forces, $N_R = 0$.

If the solution to Equation (28) is known, subject to the boundary conditions (25) and (26), the rate of collisions can be calculated from the flux of pairs through the collision surface

$$J = n_a n_b \int_{A_{coll}} (\mathbf{v}P) \cdot \mathbf{n}\, ds \qquad (29)$$

Von Smoluchowski (1917) used Equation (28) to calculate the collision rate for the limit of no bulk flow $N_{Pe} = 0$. He assumed an attractive potential only, given by

$$V_A = -\infty \qquad R \leq 1 + b/a \qquad (30a)$$

$$V_A = 0 \qquad R > 1 + b/a \qquad (30b)$$

and neglected hydrodynamic interactions. He obtained a quasi steady state collision rate, valid after a short transient:

$$J^0 = \frac{2kT}{\mu}(a+b)\left(\frac{1}{a}+\frac{1}{b}\right) n_a n_b \qquad (31)$$

The complete problem, including hydrodynamic interaction and arbitrary interparticle potential $V_T = V_T(R)$, was solved by Spielman (1970) and by Honig et al. (1971) to obtain a stability ratio for Brownian coagulation $W_{Br} = J^0/J$ of the form

$$W_{Br} = \frac{a}{b}\int_{1+b/a}^{\infty} \frac{\exp\left(\frac{V_T}{kT}\right)}{G(s)s^2}\, ds \qquad (32)$$

In the absence of Brownian motion $N_{Pe} \to \infty$, the pair probability function will ultimately attain a steady state distribution. It is anticipated that this distribution will be achieved in the time required for new particle-particle encounters. Then, $dP/dt = 0$, and the steady state solution of Equation (27) reveals that the flux of pairs through any volume contained in the region $(a+b) < r < \infty$ is a constant. If the volume is chosen to be that occupied by all trajectories that originate at $r = \infty$ and terminate at the collision surface $r = (a+b)$, then the collision rate must equal the flux at $r = \infty$ through a cross section A_I to be referred to as the upstream interception area. At $r \to \infty$, $P(\mathbf{r}, a/b) \to 1$ and $\mathbf{v} \to \mathbf{v}_o$, where $\mathbf{v}_o = \boldsymbol{\omega} \times \mathbf{r} + \mathbf{E} \cdot \mathbf{r}$, so that only the determination of A_I is needed to calculate the rate of collisions:

$$J = -n_a n_b \int_{A_I} \mathbf{v}_o \cdot \mathbf{n}\, dS \qquad (33)$$

For an attractive potential given by Equation (30) and with the neglect of hydrodynamic interactions, particle trajectories coincide with the undisturbed streamlines of the bulk motion. For shear flow, streamlines are straight, and those intersecting the collision surface define a circular upstream interception area of radius $(a+b)$. Integration of Equation (33) produces the shear induced coagulation rate of von Smoluchowski (1917):

$$J^0_{shear} = 4/3(a+b)^3 \dot{\gamma} n_a n_b \qquad (34)$$

For extensional flow, the stream function is given by

$$\psi = \dot{\gamma}\rho^2 z \qquad (35)$$

where ρ is the radial cylindrical coordinate. Streamlines are described by lines of constant stream function, and those which intersect the collision surface are given by $\psi \leq (2\dot{\gamma}/3\sqrt{3})(a+b)^3$. These streamlines define an upstream interception area which is circular and has a total surface area given by

$$A_I = \frac{8\pi}{3\sqrt{3}} \frac{(a+b)^3}{\rho} \qquad (36)$$

The radial velocity increases linearly with ρ; thus, the collision rate is finite, and

$$J^0_{ext} = \frac{8\pi}{3\sqrt{3}}(a+b)^3 \dot{\gamma} n_a n_b \qquad (37)$$

This result also applies to compressional flow, for which the streamlines are identical.

As with Brownian coagulation, the stability ratio for flow is

$$W_{flow} = J^0/J \qquad (38)$$

RESULTS

Rapid, Flow Induced Coagulation

As an improvement to von Smoluchowski's theory of rapid, flow induced coagulation, complete hydrodynamic interactions and a long-range attractive potential [Equation (3) or (4)] have been included for the determination of the upstream interception area for equal sized spheres. For shear flow, A_I was determined by retracing backwards in time the path of particles which collide after a rotation about the z axis of 180 deg. The trajectory equations (23) were numerically integrated with $N_R = 0$ and the initial conditions $\phi = 0$ deg and $R = 2$. By varying the initial conditions on θ from 0 to 90 deg, the set of trajectories was obtained which sharply defines most of the upstream interception area, as shown in Figure 4. There is, however, an additional region in which particles orbit for more than $\phi = 180$ deg before colliding. Because these additional trajectories make little contribution

to W_{flow}, only the regions for which collision occurs in rotations of $\phi \leq 360$ deg were determined, and these only for the unretarded case. These additions to the upstream interception area are shown as shaded regions in Figure 4. With A_I determined, Equation (33) was integrated and the stability ratio calculated to obtain the results presented in Figure 5.

For shear flow, these calculations are similar to those carried out by Curtis and Hocking (1970), who chose to present their results as a ratio of interception areas instead of a ratio of collision rates.

For extensional flow, a different procedure was employed. The trajectory equations (24) were numerically integrated with an upstream initial condition $R = 10$. For separations $R \geq 10$, particle-particle interactions were negligible, and the trajectories followed the undisturbed streamlines given by Equation (35). By varying the initial condition on θ, a search was performed to determine the limiting value of ψ for which collision occurred. A_I was, thereby, determined. The stability ratio for extensional flow was calculated and is also shown in Figure 5.

Similar computations for compressional flow revealed that the rapid coagulation rate is identical to that obtained in extensional flow.

Stability Criteria

The stability ratio can, in principle, be calculated for any amount of repulsion. Here, however, only those conditions were sought for which a suspension of equal sized spheres is completely stable to a given flow strength. Thus, $W_{flow} = \infty$, and the upstream interception area must vanish. For both shear and extensional flows, this requires that collision does not occur for a pair whose lines of centers are aligned with the flow at $R = \infty$.

For shear flow, the critical trajectory has the initial condition $\phi = 180$ deg, $\theta = 90$ deg, and $R = \infty$. By numerical integration of the trajectory equations, a search was performed to determine the strength of the repulsive force, as measured by N_R, necessary to prohibit coagulation at various flow strengths N_F. The results of the search are presented as a stability plane $N_R - N_F$, with the double-layer thickness and the degree of retardation as parameters. In all cases, the stability plane was divided into three regions, as shown in Figure 6. In region I, coagulation into the primary minimum is expected; in region II, secondary minimum coagulation occurs; and in region III, there should be no coagulation, the suspension being stable to flow. To aid in interpretation of Figure 6, consider a situation in which doublets are present in a quiescent suspension for, say, $N_R = 100$. If the suspension is sheared at a gradually increasing shear rate, the doublets will first deflocculate out of the secondary minimum and then coagulate into the primary minimum. At a still higher shear rate, doublets will deflocculate from the primary minimum. If the shear rate is then lowered, the dispersed suspension will again coagulate into the primary minimum. Further lowering of the shear rate will not, however, cause deflocculation or a shift to secondary minimum flocculation.

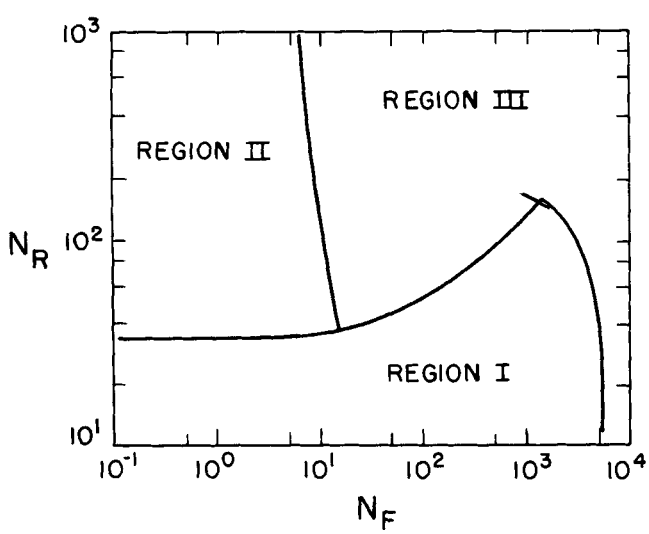

Fig. 6. Stability plane for shear flow.
Region I—primary minimum flocculation
Region II—secondary minimum flocculation
Region III—Stable.
(Calculated for unretarded attraction, constant ψ_o, $\tau = 100$, and $H_{min} = 2.004$.)

For extensional flow, the critical trajectory has the initial conditions, $\theta = 90$ deg and $R = \infty$. Because of symmetry about the x-y plane, $d\theta/dt^0 = 0$ for this trajectory, and particles approach one another until either repulsion stops them or coagulation occurs. For stability to primary minimum coagulation, dR/dt^0 must vanish at some separation for which the interparticle force is repulsive. In order for this condition to be met

$$N_F \leq \max \left[\frac{(f_A + N_R f_R)}{R} \frac{G}{(1 - \bar{A})} \right] \quad (39)$$

To determine whether deflocculation is possible, the alignment of a pair with a principal straining axis $\theta = 0$ deg is investigated. For a coagulated pair, deflocculation can only occur if $dR/dt^0 > 0$, which requires that

$$N_F > -\frac{1}{2} \min \left[\frac{(f_A + N_R f_R)}{R} \frac{G}{(1 - \bar{A})} \right] \quad (40)$$

The term in brackets may have two minima, corresponding to the primary and secondary minimum in the potential energy function.

From Table 1, the function $G/(1 - \bar{A})$ is seen to be approximately unity over the range of separation for which the interparticle force is significant. Thus the location of the approximate maxima and minima were obtained from roots of the equation

$$\frac{d}{dR} \left[\frac{f_A + N_R f_R}{R} \right] = 0$$

The stability plane $N_R - N_F$ for extensional flow divides similarly into the three regions shown in Figure 6. In all cases the shapes of the stability planes were very similar to those obtained for shear flow. By replotting the extensional flow results such that

$$N_F = 2.75\, N_{F_{ext}}$$

those portions of the stability curve which correspond to a flocculation process are nearly superposable, as shown in Figure 7. These portions of the stability curve which correspond to a deflocculation process are superposable by replotting the extensional flow results such that

$$N_F = 4 N_{F_{ext}}$$

Unless one solves the diffusion equation for arbitrary Péclet number, the influence of Brownian motion can only be incorporated in an approximate manner. The simplest method is to assume additivity of the collision rates obtained independently for flow induced coagulation and Brownian coagulation. For the case of rapid coagulation in very dilute suspensions, the experimental findings of Swift and Friedlander (1964) indicate that additivity is a good approximation. For slow coagulation, however,

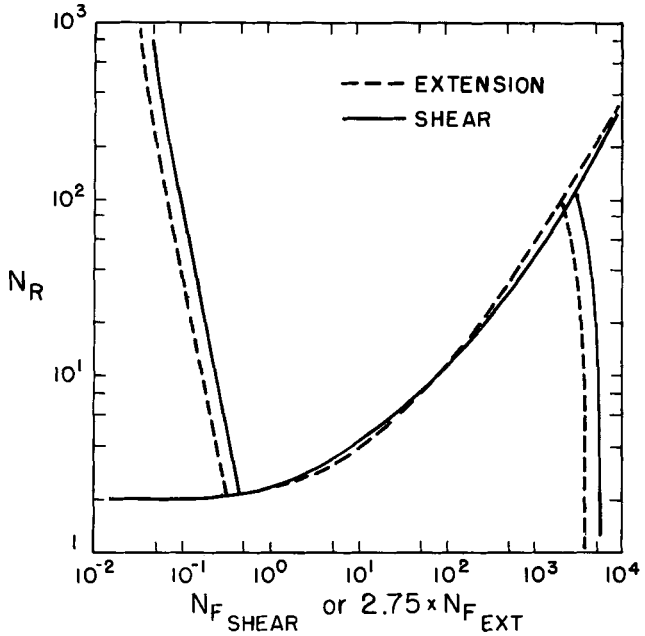

Fig. 7. Comparison of stability planes for shear and extensional flow. (Calculated for retarded attraction, $\alpha = 0.01$, constant ψ_o, $\tau = 100$, and $H_{min} = 2.004$.)

there are no experimental data to support or to refute additivity. If one assumes additivity to be valid, stability criteria for Brownian coagulation can be superposed on the criteria for flow induced coagulation.

Brownian motion has been included in our stability planes by seeking the conditions for which a suspension should be stable to primary coagulation for a period of weeks, say $W_{Br} = 10^5$. The stability ratio was calculated from Equation (32) using the value $A/kT = 1$ in the calculation of V_T. (This is the correct order of magnitude for latices.) For coagulation in the secondary minimum, we have been less precise and require only that V_{sec} be less than 1.5 kT for stability.

Stability diagrams are presented in Figures 8 through 11 for shear flow with the influence of Brownian motion included. The solid lines divide the stability plane into three regions, unless Brownian motion eliminates secondary minimum coagulation. In that case there are only two regions. The dashed lines indicate stability criteria for flow induced coagulation alone. The extensional flow results, though not shown here, are approximated by the transformations of the N_F axis previously indicated. To avoid introducing another parameter, curves showing deflocculation from the primary minimum at high shear rate are not shown but are dealt with separately.

As illustrated in Figure 6, the value of N_F at which deflocculation from the primary minimum occurs is rather insensitive to the value of N_R. Therefore, the deflocculation curve, which is nearly vertical, can be characterized by the value of N_F for $N_R = 0$ and is independent of which double-layer expression is used. The critical values of N_F for uniaxial extension were calculated from Equation (40).

TABLE 2. THE MINIMUM VALUE OF N_F NECESSARY FOR DEFLOCCULATION OF A DOUBLET IN EXTENSIONAL FLOW

$a(\mu m)$	H_{min}	$4N_{Fext}$ or N_{Fshear}
0.01	4×10^{-2}	4.8×10^1
0.1	4×10^{-3}	5.16×10^3
1.0	4×10^{-4}	5.2×10^5
10.0	4×10^{-5}	5.2×10^7

The minimum separation between particle surfaces was assumed to be 4Å, an appropriate value for particles with no adsorbed layers. Results are shown in Table 2. Because of the superposability of shear flow and extensional flow results, Table 2 also illustrates deflocculation for shear flow when $N_{Fshear} = 4N_{Fext}$.

DISCUSSION

Rapid, Flow Induced Coagulation

Hydrodynamic interactions and a long-range attractive force affect the rapid coagulation rate in opposing ways. For weak flow $N_F < 1$, the attractive force enhances the collision rate and, as observed in Figure 5, $W_{flow} < 1$. For the most part, however, the strong lubrication stresses generated at small separations diminish the collision rate and $W_{flow} > 1$. The net result for the unretarded shear flow case is that for $N_F > 10$ J is proportional to $\dot{\gamma}$ raised to the 0.77 power instead of the first power as for von Smoluchowski's result. For extensional flow, hydrodynamic interactions are less significant, and for $N_F > 10^3$, J is proportional to $\dot{\gamma}^{0.86}$.

Stability Criteria

The differences observed in Figure 2 between the forces obtained for constant surface charge and for constant surface potential are apparent from a comparison of Figures 8 and 9 (constant ψ_o) with Figures 10 and 11 (constant σ_o). In the low deformation rate limit, double-layer interactions at separations $H = 0(1/\tau)$ are sufficient to prohibit flow induced coagulation. At these separations, the differences between the force obtained for constant ψ_o and constant σ_o are small. Hence, the value of N_R necessary for stability of flow induced coagulation varies by less than a factor of 1.5 between the two cases. In the high deformation rate limit, double-layer interactions occur at much smaller separations than $H = 0(1/\tau)$. Here, the force for constant σ_o is more than an order of magnitude

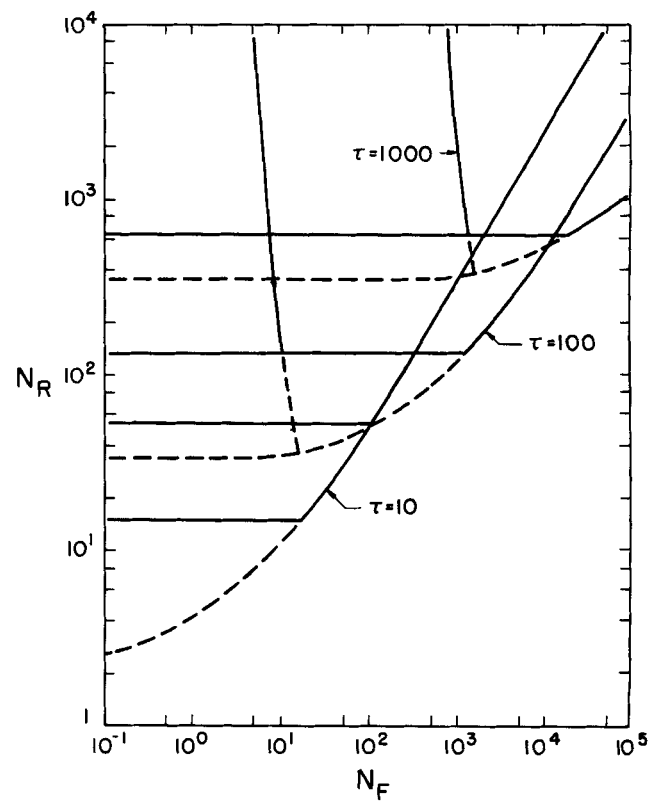

Fig. 8. Stability plane for shear flow unretarded attraction and constant ψ_o.

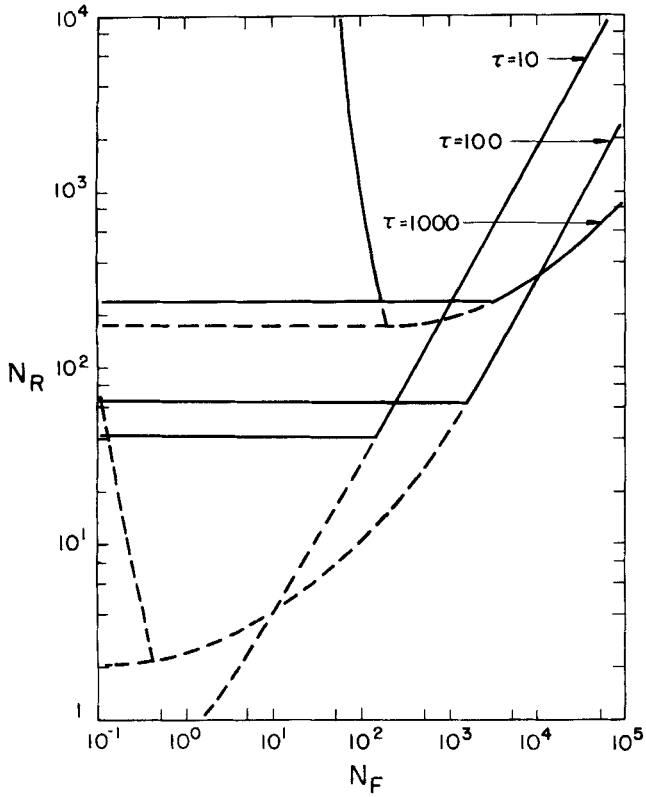

Fig. 9. Stability plane for shear flow retarded attraction, $\alpha = 0.01$ and constant ψ_o.

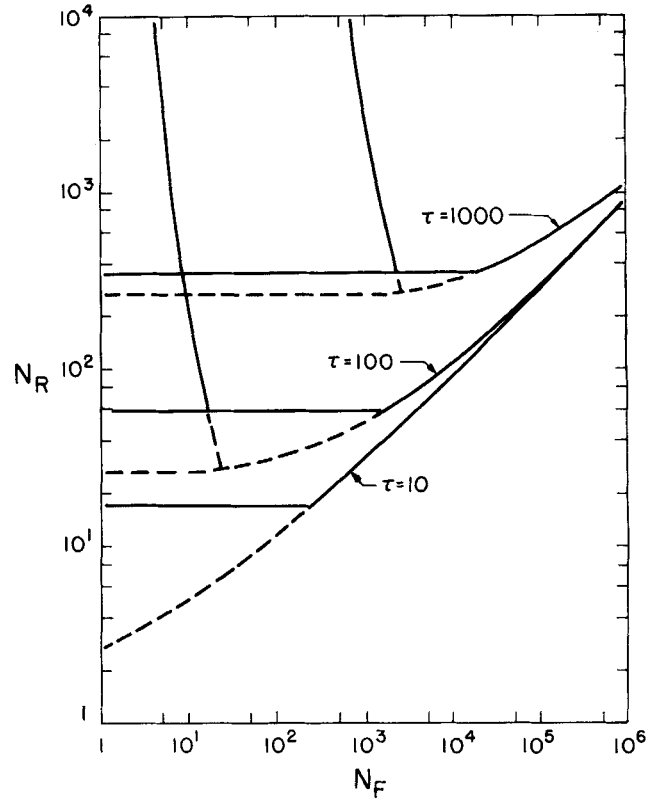

Fig. 10. Stability plane for shear flow unretarded attraction and constant σ_o.

TABLE 3. MAXIMUM VALUES FOR THE DIMENSIONLESS PARAMETERS $A/kt = 1$, $\psi_o = 100$ mV, $\lambda_L = 100$ nm, $\dot{\gamma} = 10^3$ s^{-1}, AND $\kappa = 10^7$ cm^{-1}

$a(\mu m)$	α	N_F or N_{Pe}	N_R	τ
10^{-2}	10	5×10^{-3}	2×10^2	10^1
10^{-1}	1	5×10^0	2×10^3	10^2
1	10^{-1}	5×10^3	2×10^4	10^3
10	10^{-2}	5×10^6	2×10^5	10^4

greater than the force for constant ψ_o. Thus, stability is significantly greater for the constant σ_o case. As for Brownian coagulation, a decrease in the double-layer thickness (an increase in τ) reduces the flow induced region of stability for constant σ_o. In the high deformation rate limit, however, this is not so for constant ψ_o, where stability is greater for thin double layers. This contrast between the stability results for the two surface boundary conditions, if experimentally verified, could provide insight into which double-layer expression is applicable to a given colloidal suspension.

The effect of retardation is shown in Figures 9 and 11, where $\alpha = 0.01$. For $\lambda_L = 100$ nm, this value of α corresponds to a particle size of 10 μm. Because retardation affects primarily the long-range force, stability is considerably enhanced in the low deformation rate limit, and the occurrence of secondary minimum coagulation is diminished.

Particle size is the single most important parameter governing the behavior of colloidal suspensions. Since the ratio of the hydrodynamic force to the Brownian force acting on a pair of particles is proportional to a^3, it is understandable that smaller particles are dominated by Brownian motion, while larger particles are dominated by flow. To investigate the importance of particle size, the maximum values of the parameters N_F, N_{Pe}, N_R, and τ were calculated for various particle radii. The values $A/kT = 1$ and $\lambda_L = 100$ nm were assumed together with the maximum values $\psi_o = 100$ mV, $\gamma = 10^3$ s^{-1}, and $\kappa = 10^7$ cm^{-1}, which corresponds to a 1-1 electrolyte concentration of 0.1 M. Results are shown in Table 3.

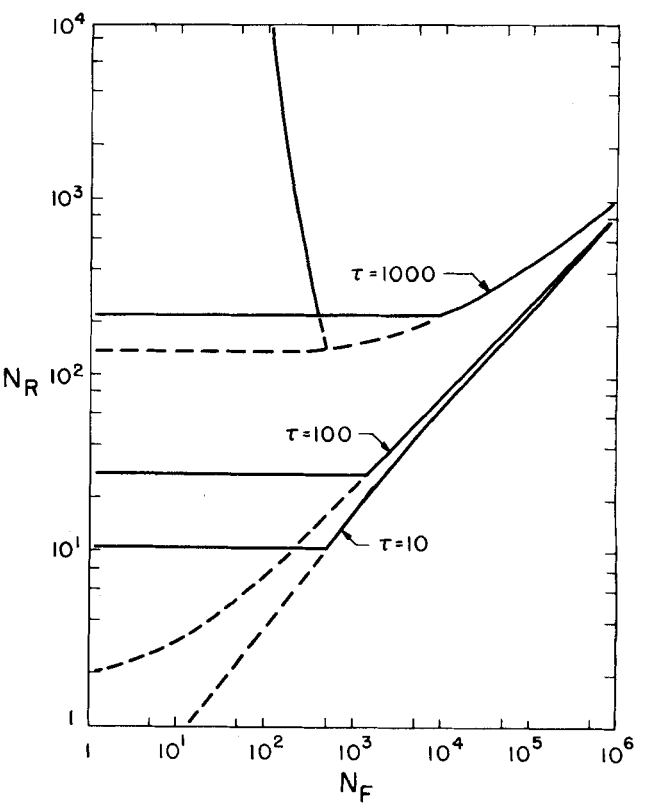

Fig. 11. Stability plane for shear flow retarded attraction, $\alpha = 0.01$ and constant σ_o.

Comparison of the maximum values in Table 3 with Figures 8 to 11 indicates that flow induced flocculation will only influence the stability criteria for particles with radii $\geq 0(1\ \mu m)$. For smaller particles, deformation rates of $10^3\ s^{-1}$ are insufficient to destabilize a suspension which is stable to Brownian motion. A comparison of the N_F values in Tables 2 and 3 furthermore indicates that deflocculation from the primary minimum is unlikely in the absence of adsorbed surfactants or macromolecules for particles of size $a \leq 10\ \mu m$.

Influence of Vorticity

From Equation (19) one sees that vorticity and deformation rate separately influence the relative velocity of a pair. The contribution to v made by vorticity is unaffected by hydrodynamic interactions and corresponds to a rigid body rotation of the pair. In shear flow this rotation decreases the time span during which hydrodynamic forces and colloidal forces interact. This effect of vorticity is found, as illustrated by the following, to decrease the efficiency of shear flow for flocculation purposes.

As a basis for comparing the efficiency of the two flows, the local bulk rate of energy dissipation is considered. It is proportional to the second invariant of the deformation-rate tensor

$$II_D = 1/4[(\text{trace } \mathbf{E})^2 + \text{trace } (\mathbf{E})^2] \qquad (41)$$

and leads to the requirement that for the bulk flows to be equivalent in their rates of energy dissipation:

$$\frac{\dot{\gamma}_{shear}}{\gamma_{ext}} = 2\sqrt{3} = 3.464 \qquad (42)$$

Since the flow induced collision rate is proportional to $\dot{\gamma}$, the two flows have the same efficiency for flocculation if for $\dot{\gamma}_{ext} = \dot{\gamma}_{shear}$

$$\frac{J_{ext}}{J_{shear}} = 3.464 \qquad (43)$$

In the absence of a long-range force and hydrodynamic interactions, the ratio of the collision rates, Equations (34) and (37), is

$$\frac{J^0_{ext}}{J^0_{shear}} = 3.628 \qquad (44)$$

Thus, extension is only 5% more efficient than shear in this case. If this 5% difference is neglected, then the stability ratios must be equal for the flows to be equivalent when particle-particle interactions are considered:

$$\frac{W_{shear}}{W_{ext}} = \frac{J_{ext}}{J_{shear}} \times \frac{J^0_{shear}}{J^0_{ext}} \qquad (45)$$

From Figure 5, $W_{shear} > W_{ext}$ for large N_F. Thus, as the effect of hydrodynamics increases in importance, shear flow becomes less efficient than extensional flow for rapid flocculation.

The influence of vorticity is also noticed in the comparison of the stability criteria for the two flows. To demonstrate this, a comparison is made of the minimum flow strength necessary for hydrodynamic forces to overcome the colloidal forces. In shear flow, the hydrodynamic forces are greatest when $\phi = 135$ and 45 deg. Here, the necessary condition for flocculation to occur is

$$N_F > 2 \max\left[\left(\frac{f_A + N_R f_R}{R}\right)\frac{G}{1 - \bar{R}}\right] \qquad (46)$$

This is not a sufficient condition, however. As the pair rotates and the hydrodynamic force decreases for $\phi < 135$ deg, it is possible that the repulsive forces will not be completely overcome, and so flocculation will not occur. For extensional flow, however, the necessary and sufficient condition for flocculation is given by Equation (39). Comparison of Equations (39) and (46) gives

$$N_{F_{shear}}/N_{F_{ext}} \geq 2$$

Since the stability criteria superpose for $N_{F_{shear}}/N_{F_{ext}} = 2.75$, it is apparent that vorticity has decreased the effectiveness of shear for flocculation and enhanced stability.

The necessary condition for deflocculation in shear is

$$N_F > -2 \min\left[\left(\frac{f_A + N_R f_R}{R}\right)\frac{G}{1 - \bar{R}}\right] \qquad (47)$$

Comparison of Equation (47) with the necessary and sufficient condition for deflocculation in extensional flow, Equation (40), gives

$$N_{F_{shear}}/N_{F_{ext}} \geq 4$$

The stability results superpose when $N_{F_{shear}}/N_{F_{ext}} = 4$. Hence the effectiveness of shear for deflocculation is unaffected by vorticity, which causes rigid-body rotation of the pair. As particles separate and rotate about one another, the colloidal forces decrease more rapidly than the hydrodynamic forces.

ACKNOWLEDGMENT

The authors wish to acknowledge partial support from the National Science Foundation under Grant GK-34427.

NOTATION

A = Hamaker constant
A_{coll} = area of the collision surface $R = a + b$
A_I = upstream interception area defined by those trajectories for which collision occurs
A_p = surface area of a particle
a, b = radius of a particle
c_i = concentration of i^{th} electrolyte
$D(r)$, $D'(R) = \frac{6\pi\mu a}{kT} D(r)$, dimensional and dimensionless relative diffusion coefficient of a pair of particles
$\mathbf{E}$ = deformation rate tensor
$\mathbf{e}_r$ = unit vector in the radial direction
e = charge of an electron
$\mathbf{F}_{Br}$ = Brownian force exerted on a pair of particles
$\mathbf{F}_c, F_c$ = interparticle force and its magnitude defined by Equation (8)
$\mathbf{F}_{hyd}$ = hydrodynamic force exerted on a particle
$f_A(r, \alpha), f_A$ = dimensionless attractive force defined by Equation (9)
$f_R(R, \tau), f_R$ = dimensionless repulsive force defined by Equation (7)
$f(r)$ = hydrodynamic function defined by Spielman (1970)
H = $R - 2$, minimum separation between particle surfaces
H_{min} = minimum value of H for which the repulsive force is finite
J^0 = coagulation rate calculated by using von Smoluchowski's attractive potential, Equations (30), and by neglecting hydrodynamic interactions
J = coagulation rate calculated by using a long-range interparticle force and by considering hydrodynamic interactions
k = Boltzmann's constant
N_F = $6\pi\mu a^3\dot{\gamma}/A$, dimensionless parameter describing the relative importance of hydrodynamic forces to attractive forces
N_{Pe} = $6\pi\mu a^3 A/kT$, Péclet number
N_R = $\epsilon\psi_o^2 a/A$, dimensionless parameter describing the relative importance of repulsive forces to attractive forces
N_o = initial number concentration of particles
N_b = total number of particles with radius b

n_a, n_b = number density of particles
$\mathbf{n}$ = outward directed normal
$P(\mathbf{r}, a/b), P$ = pair probability density function for the separation distance between the particles
p = pressure
p_o = $2\pi(R-2)/\alpha$, dimensionless parameter
$\mathbf{R}^I, \mathbf{R}^{II}$ = position vectors of the sphere surfaces relative to their respective centers
R = r/a, dimensionless separation distance between particle centers
$\mathbf{r}, r$ = $|\mathbf{r}|$, separation vector between particle centers and its magnitude
T = temperature
$\mathbf{T}_{hyd}$ = hydrodynamic torque exerted on a particle
t = time
t^0 = $\dot{\gamma}\, t$, dimensionless time
$\mathbf{U}^I, \mathbf{U}^{II}$ = translational velocity of spheres
$\mathbf{u}$ = fluid velocity
$\mathbf{u}_o$ = undisturbed fluid velocity
V_A = attractive potential energy
V_R = repulsive potential energy
V_T = total potential energy
V_{max} = maximum potential energy barrier, see Figure 1
V_{sec} = depth of secondary minimum, see Figure 1
$\mathbf{v}$ = $\mathbf{U}^{II} - \mathbf{U}^I$, relative translational velocity of a pair of particles
$\mathbf{v}_o$ = $\boldsymbol{\omega} \times \mathbf{r} + \mathbf{E} \cdot \mathbf{r}$, relative velocity of the spheres when hydrodynamic interactions vanish
$\mathbf{v}_{Br}$ = contribution to v due to Brownian forces only
$\mathbf{v}_{flow}, \mathbf{v}'_{flow} = \dot{\gamma}/a\mathbf{v}_{flow}$, dimensional and dimensionless flow contribution to v
$\mathbf{v}_{Fc}$ = contribution to v due to interparticle force only
W = stability ratio
W_{Br} = stability ratio for Brownian coagulation only
W_{flow} = stability ratio for flow induced coagulation only
x, y, z = Cartesian coordinates
z_i = valence of the i^{th} electrolyte

Script

$\mathcal{A}$ = hydrodynamic function used in Equation (19)
$\mathcal{B}$ = hydrodynamic function used in Equation (19)
$\mathcal{G}$ = hydrodynamic function used in Equation (20)

Greek Letters

α = λ_L/a, retardation parameter
∇ = gradient operator
$\dot{\gamma}$ = deformation rate
ϵ = dielectric constant
θ = angular spherical coordinate
κ = $\left[\dfrac{4\pi e^2 \Sigma c_i z_i^2}{\epsilon k T}\right]^{1/2}$, the Debye length
λ_L = London wavelength
μ = viscosity
$\boldsymbol{\sigma}$ = stress tensor
σ_o = surface charge density
ρ = $\sqrt{x^2 + y^2}$, radial cylindrical coordinate
τ = $a\kappa$, double-layer thickness parameter
ϕ = azimuthal spherical coordinate
ϕ_p = volume fraction of particles
ψ = stream function
ψ_o = surface potential
$\boldsymbol{\Omega}^I, \boldsymbol{\Omega}^{II}$ = angular velocity of spheres
$\boldsymbol{\omega}$ = angular velocity defined by Equation (12)

Roman Numerals

II_D = second invariant of $\mathbf{E}$

Subscripts

shear, ext = results pertaining to a laminar shearing flow and an extensional flow

LITERATURE CITED

Batchelor, G. K., "Brownian Diffusion of Particles With Hydrodynamic Interaction," *J. Fluid Mech.*, **74**, 1 (1976).

———, and J. T. Green, "The Hydrodynamic Interaction of Two Small Freely-Moving Spheres in a Linear Flow Field," *ibid.*, **56**, 375 (1972).

Bell, G. M., and G. C. Peterson, "Calculation of the Electric Double-Layer Force Between Unlike Spheres," *J. Colloid Interface Sci.*, **41**, 542 (1972).

Christiansen, J., "Numerical Solutions of Ordinary Simultaneous Differential Equations of the 1st Order Using a Method for Automatic Step Change," *Numer. Math.*, **14**, 317 (1970).

Curtis, A. S. G., and L. M. Hocking, "Collision Efficiency of Equal Spherical Particles in a Shear Flow," *Trans. Faraday Soc.*, **66**, 1381 (1970).

Derjaguin, B., and L. Landau, "Theory of the Stability of Strongly Charged Lyophobic Sols and of the Adhesion of Strongly Charged Particles in Solution of Electrolytes," *Acta physicochim.*, **14**, 633 (1941).

Evans, R., and D. H. Napper, "On the Calculation of the Van der Waals Attraction Between Latex Particles," *J. Colloid Interface Sci.*, **45**, 138 (1973).

Frens, G., and J. Th. G. Overbeek, "Repeptization and the Theory of Electrocratic Colloids," *ibid.*, **38**, 376 (1972).

Fuchs, N., "Über die Stabilität und Aufladung der Aerosole," *Z. Physik.*, **89**, 736 (1934).

Green, B. W., and D. P. Sheetz, "In Situ Polymerization of Surface-Active Agents on Latex Particles II. The Mechanical Stability of Styrene/Butadiene Latexes," *J. Colloid Interface Sci.*, **32**, 96 (1970).

Hamaker, H. C., "The London-Van der Waals Attraction Between Spherical Particles," *Physica*, **4**, 1058 (1937).

Honig, E. P., G. J. Roebersen, and P. H. Wiersema, "Effect of Hydrodynamic Interaction on the Coagulation Rate of Hydrophobic Colloids," *J. Colloid Interface Sci.*, **36**, 97 (1971).

Kotera, A., K. Furususawa, and Y. Kudō, "Colloid Chemical Studies of Polystyrene Latices Polymerized Without Any Surface-Active Agents II. Coagulation into Secondary Minimum," *Kolloid—Z.u.Z. Polymere*, **240**, 837 (1970).

Lifshits, E. M., "Theory of Molecular Attraction Between Solid Bodies," *Zhurnal Eksperimental'noi i Teoreticheskoi Fiziki*, **29**, 94 (1955) (in Russian).

Lin, C. J., K. J. Lee, and N. F. Sather, "Slow Motion of Two Spheres in a Shear Field," *J. Fluid Mech.*, **43**, 35 (1970).

Maude, A. D., "End Effects in a Falling-Sphere Viscometer," *Brit. J. Appl. Phys.*, **12**, 293 (1951).

Roe, C. P., and P. D. Brass, "Effect of Aliphatic Detergents on the Mechanical Stability of Polystyrene Latex," *J. Colloid Sci.*, **10**, 194 (1955).

Schenkel, J. H., and J. A. Kitchener, "A Test of the Derjaguin-Verwey-Overbeek Theory with a Colloidal Suspension," *Trans. Faraday Soc.*, **56**, 161 (1960).

Smith, E. R., D. J. Mitchell, and B. W. Ninham, "Deviations of the Van der Waals Energy for Two Interacting Spheres from the Predictions of Hamaker Theory," *J. Colloid Interface Sci.*, **45**, 55 (1973).

Spielman, L. A., "Viscous Interactions in Brownian Coagulation," *ibid.*, **33**, 562 (1970).

Stamberger, P., "The Mechanical Stability of Colloidal Dispersions," *J. Colloid Sci.*, **17**, 146 (1962).

Swift, D. L., and S. K. Friedlander, "The Coagulation of Hydrosols by Brownian Motion and Laminar Shear Flow," *ibid.*, **19**, 621 (1964).

Utracki, L. A., "The Mechanical Stability of Synthetic Polymer Latexes," *J. Colloid Interface Sci.*, **42**, 185 (1973).

Van de Ven, T. G. M., and S. G. Mason "The Microrheology of Colloidal Dispersions IV. Pairs of Interacting Spheres in Shear Flow," *J. Colloid Interface Science*, **57**, 505 (1976).

Verwey, E. J. W., and J. Th. G. Overbeek, *Theory of the Stability of Lyophobic Colloids*, Elsevier, Amsterdam (1948).

Von Smoluchowski, M., "Versuch einer mathematischen Theorie der Koagulationskinetik Kolloider Lösungen," *Z. Physik. Chem.*, **92**, 129 (1917).

Manuscript received September 2, 1976, and accepted January 5, 1977.